

The origin of high transport spin polarization in $\text{La}_{0.7}\text{Sr}_{0.3}\text{MnO}_3$: direct evidence for minority spin states

B. Nadgorny¹, I.I. Mazin¹, M. Osofsky¹, R.J. Soulen¹, Jr., P. Broussard¹, R.M. Stroud¹, D.J. Singh¹, V.G. Harris¹, A. Arsenov², and Ya. Mukovskii².

¹Naval Research Laboratory, Washington, DC 20375

²Moscow Institute of Steel and Alloys, Moscow, Russia

(November 1, 2018)

Using the point contact Andreev reflection technique, we have carried out a systematic study of the spin polarization in the colossal magnetoresistive manganite, $\text{La}_{0.7}\text{Sr}_{0.3}\text{MnO}_3$ (LSMO). Surprisingly, we observed a significant increase in the current spin polarization with the residual resistivity. This counterintuitive trend can be understood as a transition from ballistic to diffusive transport in the contact. Our results strongly suggest that LSMO does have minority spin states at the Fermi level. However, since its current spin polarization is much higher than that of the density of states, this material can mimic the behavior of a true half-metal in transport experiments. Based on our results we call this material a *transport* half-metal.

A half-metallic ferromagnet is a metal that has an energy gap at the Fermi level, E_F , in one of the two spin channels. Only the other channel has states available for transport, and thus the electric current is fully spin-polarized. Finding half-metallic or other highly spin-polarized metals would bring about major advances in magnetoelectronics, since device performance improves dramatically as the spin polarization of the metal approaches 100%.¹ Although half-metallicity has been predicted in quite a number of materials, the experimental situation is still controversial, especially for the manganese perovskite, $\text{La}_{0.7}\text{Sr}_{0.3}\text{MnO}_3$ (LSMO). Theoretical² and experimental values³⁻⁶ of the spin polarization of this fascinating material with highly unusual structural, magnetic and electronic properties, obtained by different techniques vary from 35% to 100%. Not surprisingly, when Park *et al.* concluded from their spin-resolved photoemission spectroscopy measurement that LSMO is completely spin-polarized³ it attracted immediate attention. This result was important not only from a practical viewpoint, but also as a potential new insight into the microscopic physics of this system, since the values of the spin polarization are extremely sensitive to the band structure of LSMO.⁷ The conclusion of Ref. 3, however, disagrees with the band structure calculations² which predicted only 36% for the Fermi level density-of-states (DOS) spin polarization⁸ of the bulk $\text{La}_{0.7}\text{Ca}_{0.3}\text{MnO}_3$ ($\text{La}_{0.7}\text{Sr}_{0.3}\text{MnO}_3$). Spin-resolved tunneling⁹ experiments also indicate^{4,5} incomplete (54% and 81%, respectively) spin polarization for $\text{La}_{0.66}\text{Sr}_{0.34}\text{MnO}_3$. Recent LSMO-superconductor tunneling experiments produced a spin polarization of 72%.⁶ To address this controversy, we have done systematic measurements of the transport spin polarization in $\text{La}_{0.7}\text{Sr}_{0.3}\text{MnO}_3$ single crystals and thin films using the Point Contact Andreev Reflection (PCAR) technique.

Importantly, the measured value of the spin polariza-

tion, P_n , depends on the experimental technique. It is often possible¹⁰ to define P_n in the following form:

$$P_n = \frac{\langle N_{\uparrow}(E_F)v_{F\uparrow}^n \rangle - \langle N_{\downarrow}(E_F)v_{F\downarrow}^n \rangle}{\langle N_{\uparrow}(E_F)v_{F\uparrow}^n \rangle + \langle N_{\downarrow}(E_F)v_{F\downarrow}^n \rangle} \quad (1)$$

where $N_{\uparrow}(E_F)$, $N_{\downarrow}(E_F)$ and $v_{F\uparrow}$, $v_{F\downarrow}$ are the majority and minority spin DOS and the Fermi velocities, respectively. This definition allows a direct comparison between different experiments and the theory, since all the quantities in Eq. 1 can be evaluated from the band structure. The spin polarization P_0 ($n=0$) measured by spin-resolved photoemission measurements is determined only by the DOS at the Fermi level.¹¹ Transport experiments measure a different spin polarization, which includes the Fermi velocities (Eq.1). In the ballistic, or Sharvin, limit (mean free path, L , larger than the contact size, d) the DOS is weighted linearly with v_F , and P_1 is measured.¹² In the diffusive, or Maxwell regime ($L < d$), as in the classical Bloch-Boltzmann theory of transport in metals, the weighting is quadratic in v_F ($n=2$) and P_2 is measured (assuming that the transport relaxation time, τ , is a constant). Tunneling experiments probe yet another spin polarization, P_T , which may still be formally defined using Eq.1 (for $n=2$) by replacing the velocities with spin-dependent tunneling matrix elements. It can be shown¹⁰ that for the simplest case of a specular tunnel barrier with low transparency P_T reduces to P_2 .

One can immediately see from Eq.1 that P_0 , P_1 , P_2 , and P_T can be dramatically different. In LSMO, for instance, band structure calculations predicted $P_0=36\%$, whereas $P_2=92\%$. Since the bulk current is proportional to $\langle N(E_F)v_F^2 \rangle$, $P_2=92\%$ implies that spin-majority electrons carry 96% of electric current. A system where the current is (nearly) fully spin polarized can be called a *transport* half metal, as opposed to a conventional half metal where $N_{\downarrow}(E_F) = 0$ and thus $P_0 = P_1 = P_2 = P_T = 100\%$. Our paper reports the first experimental obser-

vation of this effect.

Recently, Soulen *et al*¹³ and Upadhyay *et al*¹⁴ introduced the use of Andreev reflection for measuring transport spin polarization. The Andreev process¹⁵ allows propagation of a single electron with energy below the superconducting gap Δ from a normal metal to a superconductor by reflecting at the interface as a hole with the opposite spin. In a non-magnetic metal this process is always allowed, because every energy state of a normal metal has both spin-up and spin-down electrons. In a ferromagnet, however, the spin-up and spin-down symmetry is broken, and Andreev reflection is limited by the number of minority spin conductance channels.¹⁶ The measured degree of suppression of Andreev reflection can be then directly related to the spin polarization of the ferromagnet using an appropriately modified^{13,17} standard theory.¹⁸ This procedure allows a quantitative determination of the transport spin polarization of ferromagnetic materials.

Using this approach, we have studied thin films and bulk crystals of LSMO. The films were grown on (100)-oriented NdGaO₃, MgO, and LaAlO₃ substrates by off-axis sputtering¹⁹ and by pulsed laser deposition. The growth conditions (substrate temperature and deposition rate) were also varied to fabricate films of the same composition but with different defect concentrations, and thus different residual resistivity. The composition was determined by X-ray fluorescence with an accuracy of 5%. The crystals were grown by a floating-zone technique.²⁰

The adjustment mechanism used for the PCAR measurements and the experimental setup equipped with the standard electronics for tunneling measurements in the temperature range between 1.5 K and 4.2 K are described elsewhere¹³. Sn tips were used for all the measurements reported here. Generally, at least ten point-contact junctions were made for each sample, where the contact resistance R_n was kept within the limits $100 \Omega > R_n > 1 \Omega$, as prescribed by Ref. 21. Normalized conductance, $G(V)/G_n$, was then calculated using G_n obtained for voltages $V \ll \Delta/e$. Each normalized curve was then fitted with the model (see caption to Fig.1) to obtain the magnitude of the spin polarization.

As a further test of our technique, we measured the conductance $G(V)/G_n$ for a single contact as we cooled the LSMO samples through the superconducting transition temperature of Sn, $T_c=3.7$ K. Naturally, a strong temperature dependence of the conductance was observed as the gap opened up (Fig. 1). Each of $G(V)/G_n$ curves was then fitted independently using a modified BTK model with only two adjustable parameters: spin polarization, P and the barrier strength, Z . The value of the superconducting gap $\Delta(T)$ was determined separately from the BCS dependence. Importantly, the values of P for the same sample were practically independent of T , as expected for this temperature range, $T \ll T_{Curie}$ (see the inset in Fig. 1).

Having confirmed the consistency of our technique,

we measured the spin polarization in a number of La_{0.7}Sr_{0.3}MnO₃ thin films and bulk single crystals, whose residual resistivity ranged from 40 $\mu\Omega$ cm to 2000 $\mu\Omega$ cm (see Fig.2). Surprisingly, the transport spin polarization was greater for samples with larger residual resistivity. If the material were a true half metal, one might expect the opposite trend: better samples would have less spin-flip scattering and thus show spin polarization closer to 100%. The observed result can be understood, however, if we take into account the dependence of the transport spin polarization on the ratio of the electronic mean free path to the contact size, as discussed above. It is natural to expect that all values of the transport spin polarization, P measured for our samples should be confined between P_1 (pure ballistic limit) and P_2 (pure diffusive limit). Using the values of the densities of states [$N_{\uparrow}(E_F) = 0.58$ states/eV Mn, $N_{\downarrow}(E_F)=0.27$ states/eV Mn] and Fermi velocities ($v_{F\uparrow} = 7.4 \cdot 10^5$ m/s, $v_{F\downarrow} = 2.2 \cdot 10^5$ m/s), from Ref. 2, we obtain $P_1 = 74\%$, and $P_2 = 92\%$ in fairly good agreement with the experimental data. The last number implies that only 4% of the current is carried by the spin-minority channel, so we can assume for an estimate that the whole conductance is due to the spin-majority channel. Using Ziman's expression for conductivity,

$$\sigma_{\uparrow} = (1/3)e^2 N_{\uparrow}(E_F) v_{F\uparrow}^2 \tau_{\uparrow}, \quad (2)$$

we obtain for the three values of resistivity, $\rho \sim 40 \mu\Omega$ cm, $\rho \sim 400 \mu\Omega$ cm, and $\rho \sim 2000 \mu\Omega$ cm, the mean free paths, $L \sim 65 \text{ \AA}$, $L \sim 6.5 \text{ \AA}$, and $L \sim 1.3 \text{ \AA}$, respectively. The contact size can be estimated from the normal resistance of the contact, R_n . Using a general expression²², we can express R_n in the following approximate form:

$$R_n \approx \frac{4}{3\pi} \frac{\rho L}{d^2} + \frac{\rho}{2d} \quad (3)$$

where ρ is the residual resistivity. From Eq.3 we can find the contact size d for given values of ρ and R_n . For the lowest residual resistivity samples with $\rho \sim 40 \mu\Omega$ cm, we obtain $d \sim 35 \text{ \AA}$. Therefore, these samples are in the ballistic regime and the measured values of the transport spin polarization should correspond to P_1 . The resistivity range $\rho \sim 400 \mu\Omega$ cm corresponds to the intermediate regime ($L \sim d$), whereas the highest resistivity samples $\rho \sim 2000 \mu\Omega$ cm are in the diffusive regime ($L \ll d$), consistent with our measurements.

The theory of Ref. 18, as well as its modified version¹³, is directly applicable only to the ballistic transport case ($L \gg d$). The complete theory for an arbitrary transport regime has yet to be developed. We did derive expressions for purely diffusive regime, $L \ll d$, which will be published elsewhere.¹⁷ Importantly, when our high residual resistivity samples data were fitted with these expressions, we found that the only appreciable change was in the values of Z , while the spin polarization remained basically unchanged.

The analysis described above is based on the assumption that higher resistivity of our samples is mainly due to the increase of the number of defects and corresponds to shorter mean free path. However, higher resistivity of our samples could have also resulted from the presence of grain boundaries or some other extraneous effects. To make sure that the residual resistivity in LSMO is, indeed, controlled by the concentration of defects, we performed extended X-ray absorption fine structure (EXAFS) measurements that directly probe the local structure of a material. Specifically, the measurements on the Mn K-absorption edge give a quantitative description of the real-space local environment around the Mn cations, allowing us to reconstruct the MnO_6 octahedra in LSMO^{23,24}. Three films and the single crystal samples with the resistivity $40 \mu\Omega \text{ cm} < \rho < 800 \mu\Omega \text{ cm}$ were measured. We found that for all these samples, the MnO_6 octahedra experience little or no distortion. On the other hand, the measurements also indicate that the Mn-La/Sr bond length changes from site to site, likely due to La/Sr site defects, which are known to occur in LSMO. These differences are seen in the Mn-La/Sr correlation, where the amplitude of the Fourier peak systematically decreases with increasing residual resistivity. The change in the amplitude of this peak (while the amplitude of the nearest neighbor O peak remains unchanged) is consistent with an increase in A-site cation defects with increasing residual resistivity. This result is in agreement with the neutron diffraction refinement of LSMO samples processed under a variety of conditions that indicate the propensity for A-site defect formation.²⁵ Such defects lead to tilting and/or rotation of the octahedra, without necessarily introducing any local distortions. Defect concentrations estimated from the EXAFS correlate with the residual resistivity, demonstrating that the latter is due mainly to electron scattering by defects.

Additionally we took one of our low resistivity films and irradiated it with 10 MeV Si ions, which increased the residual resistivity. This allowed us to measure the change in the spin polarization as a function of residual resistivity in the *same* sample. We have found that the spin polarization for the irradiated sample follows the same curve (shown in Fig. 2) as for as-grown films and crystals. Although the defects in these two cases may not be of the same nature, they apparently affect the scattering rates in LSMO similarly, at least within a limited defect concentration range.

The EXAFS results analysis together with the irradiation experiment allow us to conclude that the observed universal dependence of the spin polarization on the resistivity is directly correlated with the carrier mean free path in LSMO and is not determined by the surface or morphology of the samples.

It is interesting to note that the conductivity is mostly ($\sim 95\%$) determined by the spin-majority band, while the spin polarization is controlled by the minority band. Moreover, because of the large disparity between the two bands, the same defects are likely to influence the trans-

port in the minority band stronger, as it is much easier for a minority band to approach the minimal metallic conductivity limit $k_F L \sim 1$. In this case, defects will dramatically modify the minority carrier properties, without significantly affecting the majority carrier properties. Ultimately, the minority carriers can be localized by the disorder, with the majority carriers retaining a long mean free path, to maintain overall metallic conductivity, in which case the transport spin polarization will approach 100%. Thus localization effects may be viewed as a limiting case of a transition from the ballistic to the diffusive regime. It is important to emphasize the difference between the spin polarization of the current through the interface and the spin polarization of the bulk current. While the former can change from the ballistic limit, P_1 , to the diffusive limit, P_2 , and possibly eventually to 100% if the minority carriers become fully localized, the latter is defined by the diffusive formulas even for the cleanest samples. Of course, localization affects the bulk transport spin polarization as well as the contact spin polarization.

The results of our transport spin polarization measurements for LSMO are consistent with the tunneling measurements of Refs. 4–6 and the band structure calculations², demonstrating that this material is *not* a half metal. The agreement with Ref. 2 is in fact quite remarkable, considering the approximations used in the calculations (Local Density Approximation, perfect La/Sr ordering). Some discrepancy between the theoretical prediction for the ballistic limit (74%) and our experimental values ($\sim 60\%$) is therefore not surprising (in the diffusive limit the agreement is almost perfect, $P \sim 90\%$).

How can our results be reconciled with the 100% polarization inferred from photoemission³? First, we note that our lowest resistivity films (and single crystals) are almost identical to the sample described in Ref. 3. Both have residual resistivity of $40 \mu\Omega \text{ cm} < \rho < 800 \mu\Omega \text{ cm}$, Curie temperature of $\approx 350 \text{ K}$ and coercive force of $\approx 50 \text{ G}$ (see Fig.3). On the other hand, the band structure calculations, which agree well with our measurements, predict for the photoemission-probed spin polarization, P_0 , a low number of 36%. Since only $\sim 1 \text{ nm}$ surface layer is accessible to the photoemission³, one possible resolution of this discrepancy would be that only the surface of the sample, which had undergone a complex cleaning procedure³, was half-metallic.²⁶ Indeed, it is well known that one of the main surface effects on the electronic structure is the overall band narrowing, as a surface atom has a smaller coordination number, Z , than a bulk atom (by $\approx 20\%$ for the cubic perovskite lattice). Thus the overall bandwidth, which is roughly proportional to the product Zt (t being the effective hopping), is reduced at the surface by the same amount.²⁷ As the minority band in $\text{La}_{0.7}\text{Sr}_{0.3}\text{MnO}_3$ is quite narrow and its edge is very close ($\approx 0.2 \text{ eV}$) to the Fermi energy, band narrowing can easily make the system half-metallic. To check whether a band narrowing of the order of 20% may be responsible for the results of Ref. 2, we considered another

problem, which also has band narrowing, albeit for a different reason. Namely, we calculated (in virtual crystal approximation) the effect of the uniform lattice expansion on the band structure of LSMO. This effect reduces t without changing the coordination number. We have found that just 3% linear expansion, which corresponds to approximately 10% reduction²⁸ in t , corresponding to 10% reduction in the overall bandwidth, is already sufficient to make the system half-metallic²⁹. Therefore, it is quite plausible that the surface layer of LSMO is, indeed, half-metallic.

Another possible explanation of the photoemission results can be attributed to the spin-filtering, whereby a faster scattering rate for minority spin electrons compared to the majority spin electrons leads to an excessive apparent spin polarization.³⁰ This explanation is also consistent with the lack of dispersion $E(k)$ observed in Ref. 3.

In conclusion, our results unambiguously show the presence of the minority electrons at the Fermi level in the bulk of LSMO, in good agreement with the band structure calculations², indicating that this material is not a half-metal. At the same time our measurements have directly shown a high degree of the current spin polarization ($58\% < P < 92\%$) in bulk LSMO. This result confirms that this material is a promising candidate for magnetoelectronics applications, since ultimately it is the current spin polarization that controls the performance of these devices. One can call $\text{La}_{0.7}\text{Sr}_{0.3}\text{MnO}_3$, therefore, a *transport* half-metallic ferromagnet, due to the fact that the spin polarization of the current in this material is approaching 100% in the high resistivity limit. The origin of this high current spin polarization is, however, entirely different from that in the case of a conventional half-metal. It is mostly due to the large difference in the mobility of the spin-up and spin-down electrons, rather than their DOS. Our conclusions are based not just on the measured spin-polarization values themselves, but rather on the observation of a clear correlation between the bulk resistivity and the measured spin polarization which is *opposite* to the one expected for a true half-metal.³¹ This picture agrees quite well with the band structure calculations, and the results of the tunneling studies for this complex and remarkably rich material system.

The authors are grateful to T. Geballe, D. Worledge, and I. Zutic for useful discussions.

¹ G.A. Prinz, Phys. Today, **48** 58-63 (1995); Science, **282**, 1660 (1998).

² W.E. Pickett and D.J. Singh, Phys. Rev. **B53**, 1146

³ J.-H. Park, E. Vescovo, H.-J. Kim, C. Kwon, R. Ramesh, and T. Venkatesan, Nature, **392**, 794 (1998).

⁴ Yu Lu, X. W. Li, G. Q. Gong, Gang Xiao, A. Gupta, P. Lecoeur, J. Z. Sun, Y. Y. Wang, and V. P. Dravid, Phys. Rev. **B54**, R8357 (1996).

⁵ J.Z. Sun, L. Krusin-Elbaum, P.R. Duncombe, A. Gupta, R.B. Laibowitz, Appl. Phys. Lett. **70**, 1769 (1997).

⁶ D.C. Worlege and T.H. Geballe, Appl. Phys. Lett., **76**, 900 (2000).

⁷ In an idealized double exchange system Hund's rule coupling is much stronger than the hopping amplitudes, and hence the exchange splitting is much larger than the bandwidth. Obviously, such a system is always a half-metal. LSMO, however, is far from this idealized picture, and the two energy scales are comparable. In such a situation, whether or not the material is half-metallic depends intimately on the details of its electronic structure.

⁸ In Ref.² only $\text{La}_{2/3}\text{Ca}_{1/3}\text{MnO}_3$ compound was considered. We have done a few additional calculations for $\text{La}_{2/3}\text{Sr}_{1/3}\text{MnO}_3$ and found that substituting Sr for Ca practically does not change the results.

⁹ M. Juliere, Phys. Lett., **54A**, 225 (1975).

¹⁰ I.I. Mazin, Phys. Rev. Lett, **83**, 1427 (1999).

¹¹ In the constant matrix element approximation.

¹² Yu.V. Sharvin, Sov. Physics JETP **21**, 655 (1965).

¹³ R.J. Soulen Jr., J.M. Byers, M.S. Osofsky, B. Nadgorny, T. Ambrose, S.F. Cheng, P.R. Broussard, C.T. Tanaka, J. Nowak, J.S. Moodera, A. Barry, J.M.D. Coey, Science, **282**, 85-88 (1998).

¹⁴ S.K. Upadhyay, A. Palanisami, R.N. Louie, and R.A. Buhrman, Phys. Rev. Lett. **81**, 3247 (1998).

¹⁵ A. F. Andreev, Sov. Phys. JETP **19**, 1228 (1964).

¹⁶ M.J.M. de Jong and C.W.J. Beenakker, Phys. Rev. Lett. **74**, 1657 (1995).

¹⁷ I.I. Mazin, A.A. Golubov, and B. Nadgorny, cond-mat/0010326

¹⁸ G. E. Blonder, M. Tinkham, and T.M. Klapwijk, Phys. Rev. **B 25**, 4515 (1982).

¹⁹ P.R. Broussard, S.Q. Qadri, V.M. Browning, and V.C. Cestone, Appl. Surf. Sci. **115**, 80 (1997).

²⁰ D. Shulyatev, S. Karabashev, A. Arsenov, and Y. Mukovskii, Journ. of Crystal Growth, **199**, 511 (1999).

²¹ G. E. Blonder and M. Tinkham, Phys. Rev. **B 27**, 112 (1983).

²² G. Wexler, Proc. Phys. Soc. London **89**, 927 (1966).

²³ The fine structure data extending from $\sim 30\text{eV}$ to 800 eV beyond the Mn absorption edge were collected at room temperature in fluorescence mode using a dynamic flow N gas ionization detector equipped with Soller slits and a 6 μm Cr filter. Measurements were performed using beam line X23B at the National Synchrotron Light Source (Brookhaven National Laboratory, Upton, NY) with a storage ring current of 200-250 mA and an energy of 2.5 GeV. EXAFS data were analyzed following standard procedures leading to the Fourier transformation. Modeling of the near neighbor Mn-O bonds was performed using the FEFF simulation codes of Ref. 24.

²⁴ J.J. Rehr, S.I. Zabinsky, and R.C. Albers, Phys. Rev. Lett., **69**, 33997 (1992).

²⁵ J.F. Mitchell, D.N. Argyriou, C.D. Potter, D.G. Hinks, J.D. Jorgensen, S.D. Bader, Phys. Rev. **B 54**, 6172 (1996).

²⁶ As PCAR is probing the depth of the order of the mean

free path it is much less sensitive to the surface electronic structure.

²⁷ Such effects as surface relaxation change hopping integrals t , thus partially offsetting the reduction of the coordination number. However, the net effect on the total bandwidths is usually negative.

²⁸ According to the Harrison scaling rule, the pd hopping scales with the bond length, a , as $a^{-3.5}$ (W.A. Harrison, *Electronic Structure and the Properties of Solids*, W.H. Freeman and Co., San Francisco, 1980).

²⁹ Note that in layered perovskites, where the bandwidth is due predominantly to the in-plane hopping, one does *not* expect surface band narrowing, and, indeed, *ab initio* calculations show very small surface effect in layered $\text{LaSr}_2\text{Mn}_2\text{O}_7$ [P.K. de Boer, R.A. de Groot, Phys. Rev. **B**

60, 10758 (1999)].

³⁰ D.R. Penn, P.S. Apell, S.M. and Girvin, Phys. Rev. Lett. **55**, 518, 1985; D.P. Pappas, Phys. Rev. Lett. **66**, 504, 1991.

³¹ It is probably impossible to measure exactly 100% spin polarization using the PCAR technique even in a true half metal, due to potentially always-present spin-flip processes. However, the normalized conductance, $G(0)/G(V)$, measured in our “defect-free” low resistivity LSMO sample $G(V)/G(0)$ (corresponding to $\sim 60\%$ spin polarization) differs by a factor of 5 from $G(0)/G(V)$ for the sample with the highest polarization measured to date by this technique ($\sim 95\%$ in CrO_2), indicating a profound difference between the two materials.

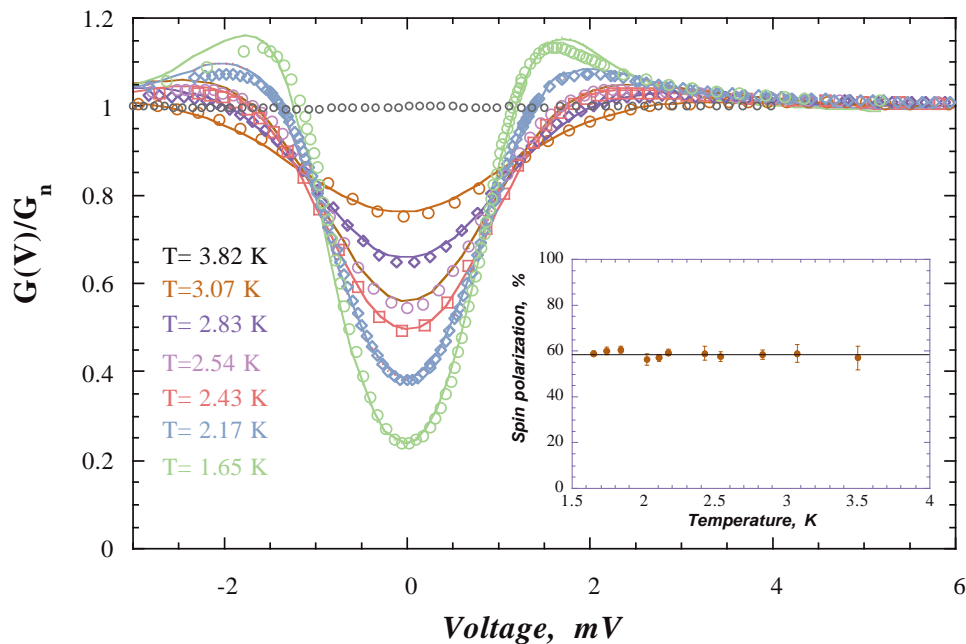


FIG. 1. Experimental data and fits at different temperatures for a $\text{La}_{0.7}\text{Sr}_{0.3}\text{MnO}_3$ film. The experimental data were corrected for the lead resistance and small non-linearity in I-V characteristics above the gap. The normalized $G(V)/G_n$ curves were fitted for all temperatures, varying the spin polarization, P and the barrier strength, Z . The BCS temperature dependence for the superconducting gap $\Delta(T)$ was used. Inset: Temperature dependence of the spin polarization values for the same sample for $1.6 \text{ K} < T < 4.2 \text{ K}$.

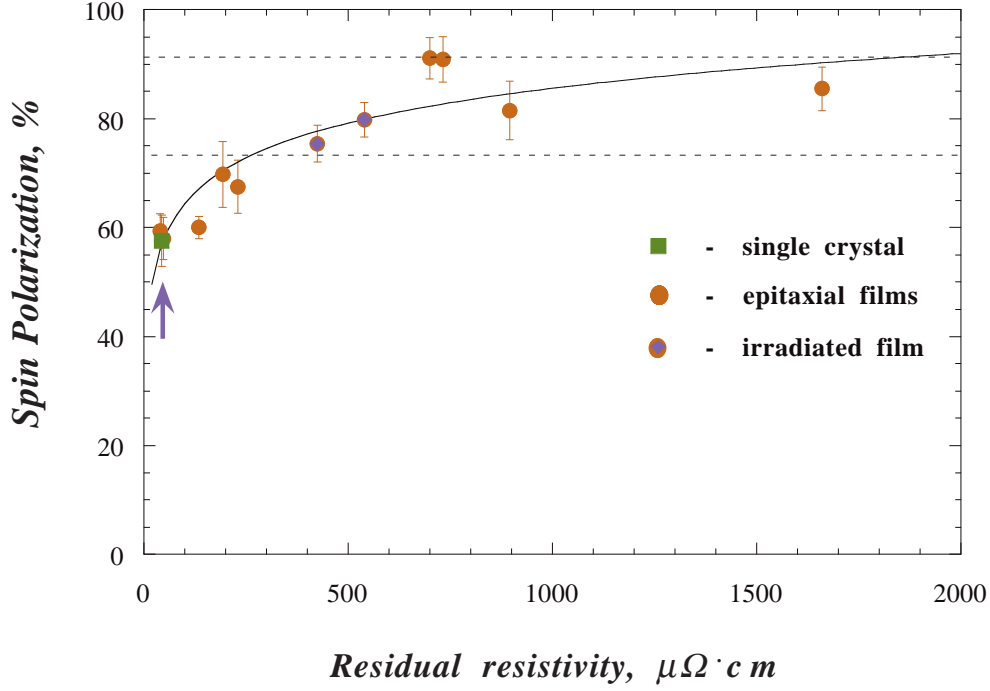


FIG. 2. Spin polarization as a function of the residual resistivity of $\text{La}_{0.7}\text{Sr}_{0.3}\text{MnO}_3$ films and single crystals at $T=1.6$ K. The arrow indicates the lowest resistivity film that was later irradiated with Si ions (the higher resistivity film corresponds to the higher dose). Dashed lines correspond to $P_1=74\%$ and $P_2=92\%$ (see text). Solid line is a guide to the eye.

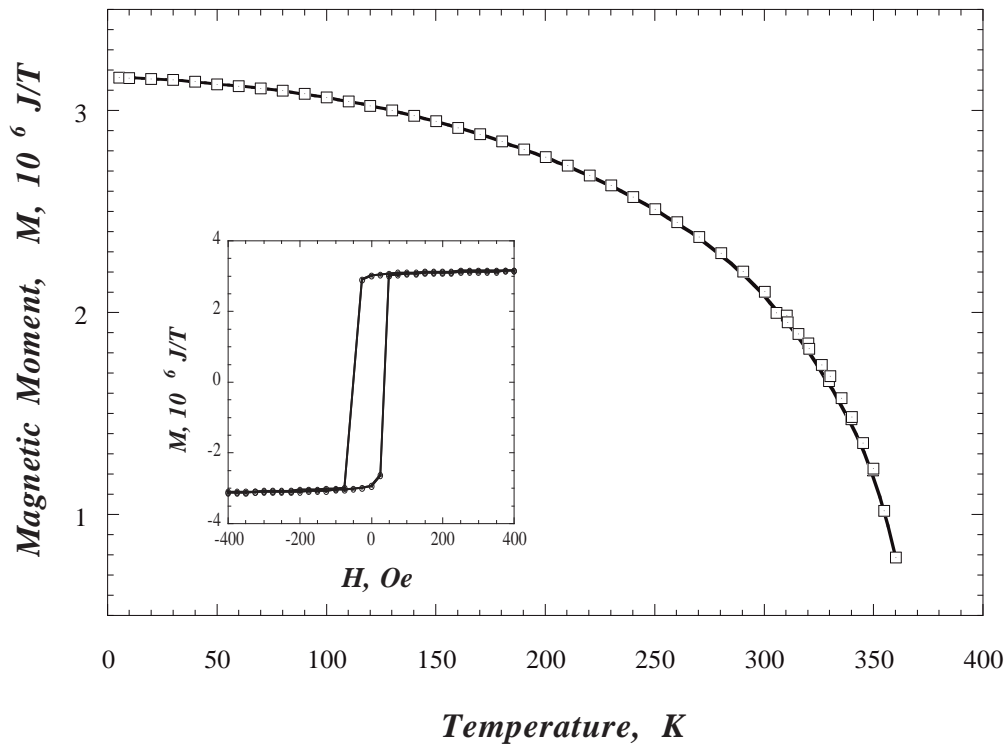


FIG. 3. Temperature dependence of the magnetic moment of the lowest resistivity film in the external in-plane field of 500 Oe. Inset: Hysteresis loop for the same film at $T=4.2 \text{ K}$.